ATMOSPHERIC SCIENCE LETTERS
Atmos. Sci. Let. **10**: 267–272 (2009)
Published online 28 October 2009 in Wiley InterScience
(www.interscience.wiley.com) **DOI:** 10.1002/asl.238

The neighbor enclosed area tracking algorithm for extratropical wintertime cyclones

Masaru Inatsu*
Graduate School of Science, Hokkaido University, Sapporo, Japan

Correspondence to: Masaru Inatsu, Graduate School of Science, Hokkaido University, Rigaku-8th bldg., N10W8, Kita, Sapporo 0600810 Japan. E-mail: inaz@mail.sci.hokudai.ac.jp

Received: 6 May 2009
Revised: 15 August 2009
Accepted: 15 August 2009

Abstract

The neighbor enclosed area tracking (NEAT) algorithm is proposed as an alternative method to conventional point-to-point cyclone tracking approaches. NEAT enables us to count the genesis and tracks of individual cyclones as well as the number of merged and separated cyclones. Little difference in cyclone genesis or track climatology in the Northern Hemisphere was found between NEAT and conventional tracking. The NEAT results indicate a high probability of cyclone merger in the western Pacific and western Atlantic. Composite maps and backtracking from merged cyclones reveal the characteristics of merged cyclones.

Keywords: **storm tracking; cyclone merger; connected-component labeling**

1. Introduction

Since the replacement of manual synoptic-chart analysis with semi-objective automated algorithms (e.g. van Bebber, 1891), Lagrangian storm tracking has been widely recognized as an effective approach for analyzing detailed statistics of extratropical weather systems (see Ulbrich *et al.*, 2009 for a comprehensive review). In contrast to the conventional Eulerian approach requiring calculation of the variance or covariance of filtered climatic variables (Blackmon, 1976), the Lagrangian approach provides information on the preferred locations of cyclone genesis and lysis, the average moving speed and lifetime of weather systems, and the difference between cyclone and anticyclone statistics. With advances in computer resources in recent decades, researchers have developed state-of-the-art automatic algorithms (Lambert, 1988; Le Treut and Kalney, 1990; Murray and Simmonds, 1991; Sinclair, 1994; Hoskins and Hodges, 2002) to track cyclones on a gridded map. These algorithms can be applied to reanalysis data or numerical model outputs and have recently been used in global warming studies (e.g. Bengtsson *et al.*, 2009).

Most automated Lagrangian tracking algorithms contain three procedures: cyclone identification, cyclone tracking, and quantification of cyclone intensity and activity (Ulbrich *et al.*, 2009). Initially, cyclone identification was simply based on a comparison of neighboring grid points of sea-level pressure (SLP) data (Lambert, 1988; Le Treut and Kalney, 1990). Murray and Simmonds (1991) proposed a subsequent iterative search approach using the SLP, SLP gradient, and Laplacian of SLP to detect not only slow-moving closed-contour pressure minima but also fast-moving open-contour pressure depressions. As SLP is better for capturing the low-frequency margin of the synoptic range (Hodges *et al.*, 2003), low-level vorticity has often been used alternatively (e.g. Sinclair, 1994; Hodges, 1994), although vorticity tracks tend to emphasize high-frequency characteristics. Hoskins and Hodges (2002) showed tracks not only for SLP or vorticity but also for meridional wind, potential temperature, or potential vorticity. They additionally applied a spatial filter before cyclone identification to effectively eliminate the influence from the background flow as well as bogus low-pressure data above mountains and plateaus. Hodges (1994) used the connected-component labeling (CCL) technique (Samet, 1989) to detect the 'central' point as the centroid of a region satisfying a particular condition, instead of finding the local-minimum point. Wernli and Schwierz (2006) proposed another scheme for detecting closed contours of SLP for cyclone identification. The next procedural development, called cyclone tracking, mainly employed a near-neighbor point search to neighbor-time cyclone-center datasets. Murray and Simmonds (1991) used past motion and the pressure tendency to identify which of several near-neighbors was most likely to be the next position of a cyclone. Sinclair (1994) minimized a cost function involving motion, pressure, and vorticity tendencies in cyclone tracking. Many schemes exclude very short-lived tracks with a 1-day lifetime threshold. Finally, cyclone intensity and activity are mainly quantified as cyclone track density, and other accompanying products such as genesis and lysis densities, mean lifetime, average moving vector, and mean growth rate can also be obtained (e.g. Hoskins and Hodges, 2002).

In principal, the above neighbor-point tracking (NPT) methods identify more cyclone centers from higher resolution data (*cf.* Blender and Schubert, 2000; Pinto *et al.*, 2005). Because tracking using latitude–longitude gridded data may unrealistically feature too many cyclone tracks in higher latitudes, preprocessing to smooth data should be applied before cyclone identification (Sinclair, 1997). Moreover, as described above, pressure and vorticity tend to emphasize lower and higher frequency features, respectively. Cyclone identification in NPT procedures hence depends on the data resolution of the target variable.

A crucial problem in NPT is its requirement of some complicated connecting conditions for near-neighbor tracking. In near-neighbor tracking, two neighboring points are connected (disconnected) when they satisfy (violate) conditions based on the distance between them. The number of tracks depends on the distance. It is also particularly difficult (or rather, subjective) for NPT schemes to detect whether more than two points in a particular time frame merge into a single point in the following time frame, and vice versa. Furthermore, NPT prevents us from estimating the shape of cyclones and the transport of material or dynamical quantities by an individual eddy, as the cyclone track is determined based on points.

This paper introduces neighbor enclosed area tracking (NEAT), an alternative technique to the NPT approach. The NEAT technique easily decreases the effect of data reduction without an additional filtering of cyclone identification and uses a simpler connecting condition for cyclone tracking. Moreover, NEAT has the ability to produce fruitful information on cyclone mergers and separations, cyclone shape, and material transport by individual eddies (the latter two features will be reported elsewhere).

It is known that if two cyclones pass, respectively, over the north and south of Japan, they frequently merge in the western Pacific (Ogura *et al.*, 2006; an example is shown in Figure 2a and b). For such cases, the southern cyclones tend to be stimulated just above the sea surface temperature front to the north of oceanic western boundary currents (Xie *et al.*, 2002), whereas the northern cyclones, moving eastward along the polar front jet, are connected to potential vorticity disturbances in the upper troposphere (Takayabu, 1991). In these regions, cyclones often merge and then rapidly develop. However, although Dean and Bosart (1996) reported the climatologies of trough merger based on NPT, merged cyclones have not yet been described in a climatological sense using an objective tracking algorithm. This has prevented the calculation of merged cyclone climatology, investigation of the average growth rate, and backtracking from the point of merger. This study focuses on statistics for merged cyclones in both the western Pacific and the western Atlantic to demonstrate the potential of the NEAT method (see Section 4).

2. Methodology

The data used were 6-h Japanese 25-year reanalysis (JRA25)/Japan Meteorology Agency Climate Data Assimilation System (JCDAS) gridded data from January 1979 to December 2008 with 1.25° latitude by 1.25° longitude resolution (Onogi *et al.*, 2007). Similar to the NPT method, the NEAT scheme consists of a preprocessing step and three subsequent procedures: cyclone identification, cyclone tracking, and cyclone track quantification.

First, following Hoskins and Hodges (2002), we used meridional wind at 850 hPa (V850) that had a medium-frequency peak in the synoptic range. For the preprocessing, we employed a temporal filter to the V850 data to select synoptic-scale eddies with a period less than 10 days. Note that this preprocessing unintentionally contributes to reducing the resolution problem.

NEAT completes cyclone identification and cyclone tracking in a single process of equivalent labeling for spatiotemporally connected domains [a similar idea was used in the satellite cloud image analyses of Vila *et al.* (2008) and Morel and Senesi (2002)]. We first feature grids that satisfy a particular condition. The condition used here was that filtered V850 data were >10 m s^{-1}, with almost $+2$ standard deviations, in the 20°N–60°N zonal belt; approximately 2–3% of grid points met this condition. The CCL first applies the same label to neighboring spatial grids satisfying the condition (Samet, 1989; Hodges, 1994). If we regard Figure 1 as horizontal graphs, we can see that two connected images are present in this example; the northern and southern images are labeled 1 and 2, respectively. To reduce the resolution problem, we simply discarded connected areas of less than 19 286 km^2, equivalent to two grids on the equator and about four grids at 60°N. Expanding on Hodges' (1994) approach, the CCL technique was next applied to consecutive time frames. If two images in a neighboring time frame overlap, the CCL gives them the same label; otherwise, the images are given different labels. In Figure 1, the first and last times for the connected image were considered to represent genesis and lysis, respectively (highlighted regions in Figure 1b). Here, merger is defined as the situation in which more than two separated images in a certain time frame overlap a single connected area in the next time frame (light shading in Figure 1b). Separation is defined as the situation in which a single connected area in a time frame overlaps more than two separated areas in the next time frame (dark shading). Moreover, since the temporal resolution of the dataset was somewhat sparse, the original image was shifted 2 ± 2 grids in longitude and 0 ± 1 grid in latitude for the temporal connected-domain labeling. However, this procedure is unnecessary if a dataset has ample temporal resolution. We consider the NEAT method to give a simpler and more unifying condition than NPT approaches for cyclone identification and tracking.

Finally, NEAT quantifies cyclone track activity. NEAT outputs are different from those of NPT, as

DOI: 10.1002/asl

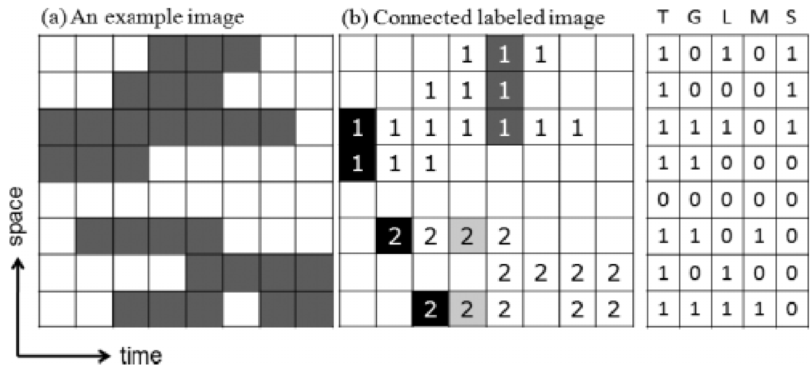

Figure 1. (a) An image of spatiotemporal grid data. Shaded areas satisfy the condition set in the NEAT algorithm. (b) The connected labeled image of (a). Highlighted areas denote cyclone genesis and lysis; areas with light and dark shading denote merged and separated grids, respectively. Total track, genesis, lysis, merged, and separated numbers are shown in the columns labeled T, G, L, M, and S, respectively, in the right of the panel.

every image has the particular domain where a condition is satisfied. Discarding parameters of the influential domain to calculate tracking statistics, the NEAT method simply calculates the track number that shows how many cyclone tracks pass over every grid (the column labeled T at the top of Figure 1b). Similarly, the genesis, lysis, merger, and separation numbers show how many cyclones are born, die, merge, and separate (columns G, L, M, and S, respectively). The growth rate was also measured as the time derivative of featured areas.

Figure 2 shows a synoptic-chart example for merger and separation, both of which were newly calculated using the NEAT approach. The synoptic chart just before a merger case at 18Z 23 January 2008 shows two cyclones over the north and south of Japan (Figure 2a). Two areas with the same label were separated at that time. After the merger, two SLP centers approached each other, and a single equivalently labeled area was found (Figure 2b). The two SLP centers were merged and deepened at 12Z 24 January 2008 (data not shown). This represents a typical merger case (Ogura *et al*., 2006). In contrast, the situations of separation appear to be rather diverse; here, one example is presented for the central North Pacific at 18Z 10 January 2008. Before separation, two SLP systems around 55°N and 40°N were close, and an equivalently labeled area was formed (Figure 2c). The two SLP systems as well as the equivalently labeled area then separated (Figure 2d) because the northern system kept its position while the southern system moved eastward.

3. Global climatology

The contours in Figure 3a show the December–January–February (DJF) climatology of the track number. Two clear maxima, in both the Pacific and Atlantic, correspond to two major storm tracks during Northern Hemisphere winter; this result is consistent with findings from conventional Eulerian approaches (Blackmon, 1976). The track number also shows many

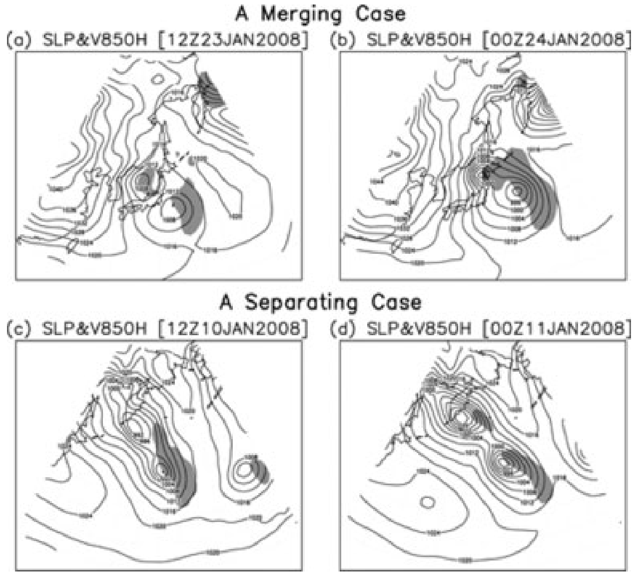

Figure 2. Synoptic charts (a) before and (b) after a merger case at 18Z 23 January 2008 and (c) before and (d) after a separation case at 18Z 10 January 2008. Contours show SLP at intervals of 4 hPa and shadings show CCL areas that satisfy the condition of >10 m s^{-1} high-pass-filtered meridional wind at 850 hPa.

minor tracks between the Mediterranean and Middle East, across Northern Siberia, between the Mongolian Plateau and the Sea of Japan, and between Alaska and the Great Lakes, all of which were similarly calculated by other track algorithms (e.g. Hoskins and Hodges, 2002).

The shaded areas of Figure 3a show the climatological genesis number in DJF. At the beginning of the Pacific storm track, the local genesis maxima are located Northeast of China, around the mouth of the Yangzi River, and east of Japan. This result is consistent with that of Adachi and Kimura (2007) who suggested that cyclones around Northeast Asia tend to be generated in these limited regions. At the beginning of the Atlantic storm track, the genesis maxima are located in Southern Alaska, the central Rockies, and the mouth of Saint Lawrence River, as shown by the genesis density based on vorticity data (Hoskins and

DOI: 10.1002/asl

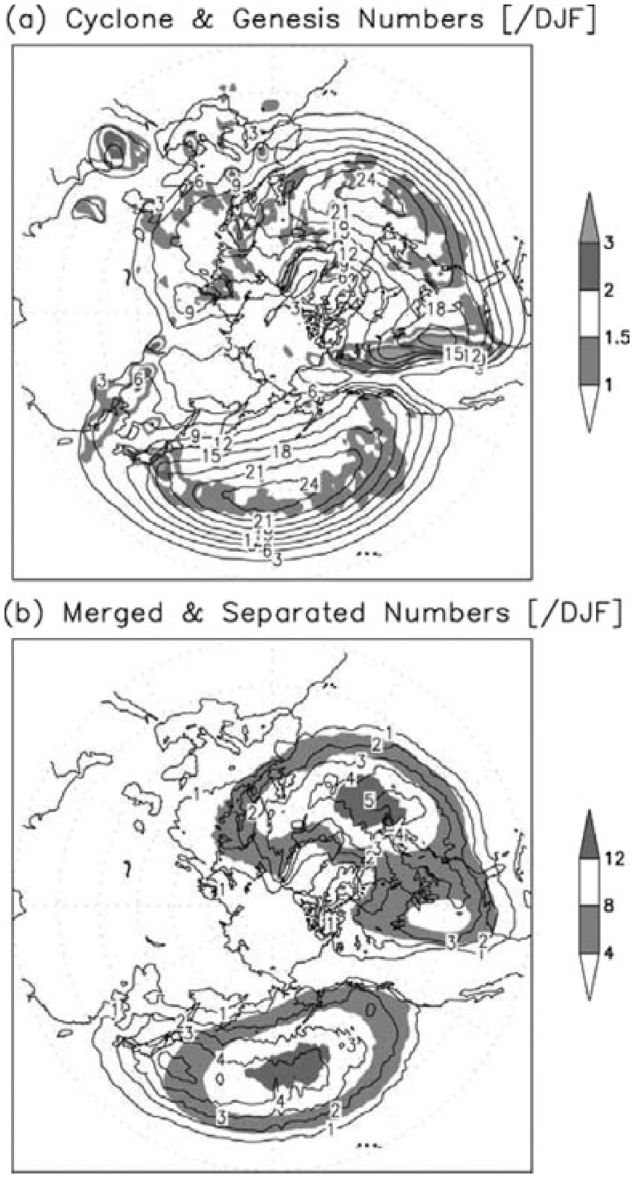

Figure 3. The DJF climatology of (a) track number (contour; interval is three times per DJF) and genesis number (shading, described on the right-hand side of the figure; unit is times per DJF) and (b) merged number (contour; interval is 1) and separated number (shading), based on JRA25/JCDAS data from January 1979 to December 2008.

Hodges, 2002). A large genesis value is also found in the two major tracks as well as most of the minor tracks.

Figure 3b shows the DJF climatology of merged and separated cyclone numbers. There are more than four merged cyclones in the DJF season in the eastern part of the two major tracks [120 °E–180 °E and 25°N–45°N for the Pacific (Region P) and 80 °W–20 °W and 35°N–55°N for the Atlantic (Region A)]. In particular, the merged numbers attain a maximum just east of Japan [140 °E–160 °E and 30°N–40°N (Region J)] and Newfoundland [60 °W–40 °W and 40°N–50°N (Region C)]. The merged cyclone statistics are the main focus of the next section. Two local maxima in the separated number are located in the central Pacific and central Atlantic. In these regions, there are more than 12 separated cyclones, representing approximately half of the track number. This is probably because, during the occlusion stage of a cyclone, the featured domain may be distorted allowing minor fragments to separate from the main body of the eddy. Image shape indices obtained by NEAT allow for quantitative discussion of eddy distortion (Thorncroft *et al.*, 1993).

4. Merged cyclone analysis

Using the NEAT technique, this study determined the season in which cyclones are most likely to merge and examined whether merged cyclones show more rapid development than non-merged cyclones. Preferred passage routes were also examined for merged cyclones in Regions J and C.

Figure 4a shows the seasonal variability of merged cyclone numbers in Regions P and A. The figure indicates that, in both regions, merger often occurs in the cold season. Furthermore, a relative minimum is shown in Region P, in accordance with the North Pacific mid-winter suppression as described by Nakamura (1992). Figure 4b and c presents the probability density functions (PDFs) for the maximum growth rates of merged and non-merged cyclones in Regions P and A. The PDF distribution for the non-merged cyclones is almost normal with average values of 1.62 in Region P and 1.71 in Region A. Merged cyclones, with a growth rate of less than 1.5 times the maximum

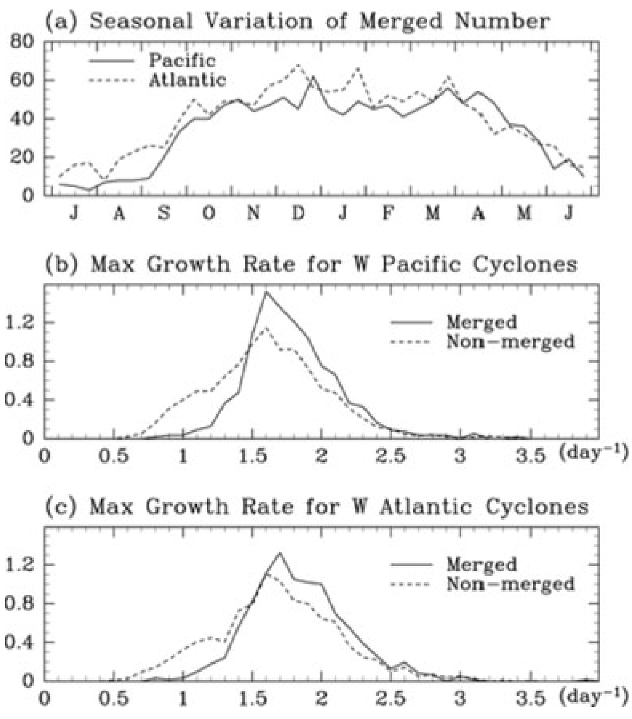

Figure 4. (a) Seasonal variability of merged cyclone numbers (solid line) in Region P (120 °E–180 °E and 25 °N–45 °N) and (dotted line) Region A (80 °W–20 °W and 35 °N–55 °N). PDF of the maximum growth rate (time per day) for merged cyclones (solid line) and non-merged cyclones (dotted line) in (b) Region P and (c) Region A.

per day, are less likely to form in both regions, even though both have similar positive distribution tails. With a 99% confidence level, the averaged maximum growth rate for the merged cyclones is approximately 10% greater than that for the total cyclone number.

Figure 5 shows backtracked cyclone genesis and backtracked track numbers in Regions J and C. Cyclones with lifetimes >1 day before merger were composited. In the western Pacific, both genesis numbers and track numbers increase from east of China to Region J. Cyclone numbers in the Sea of Japan and southwest of Japan are slightly larger than from South Korea to central Japan. This indicates that passage to the north and south of the Japan Islands is preferable for merged cyclones from Region J (*cf.* Figure 2a and b). In the Atlantic, the track number in the backtracking is relatively high from the regions north and south of the Rockies to Region C. A local cyclone genesis maximum is also located around the state of Virginia. This suggests that cyclone paths from north of the Rockies and from south of the Rockies or Virginia might typically be merged.

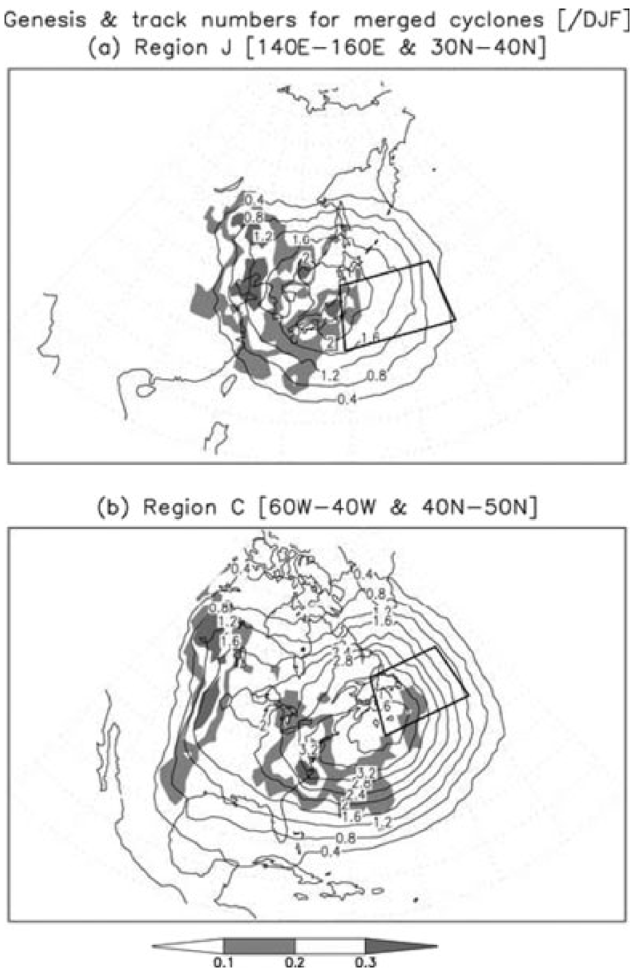

Figure 5. Composite maps of track number (contour; interval is 0.4) and genesis number (see reference at the bottom of the figure) for merged cyclones in (a) Region J (140 °E–160 °E and 30 °N–40 °N) and (b) Region C (60 °W–40 °W and 35 °N–45 °N). A solid rectangle denotes Regions J or C in each panel.

5. Concluding remarks

The NEAT algorithm introduced here is an alternative method for tracking cyclones. NEAT provides the numbers of not only cyclone tracks and geneses but also merged and separated cyclones. Using the NEAT algorithm, this study has statistically shown that the maximum growth rate of merged cyclones is greater than that of non-merged cyclones. Furthermore, the high probability of cyclone merger coincides with the seasonally varying total storm-track activity. In addition, the results reveal two preferred cyclone pathways prior to cyclone merger.

Statistics for merging cyclones may be extended to interannual variability as well as to global warming projections. Assuming that cyclone merger happens with a constant probability, storm activity should be in phase with the maximum merger number, even in its interannual variability. Global warming is expected to weaken storm activity (Ulbrich *et al*., 2009; Inatsu and Kimoto, 2005), which would decrease cyclone merger around the western Pacific. The use of NEAT to examine cyclone merger in the Southern Hemisphere would allow for an interesting comparison with cyclone merger in the Northern Hemisphere (*cf.* Sinclair, 1994; Hoskins and Hodges, 2005).

A three-dimensional extension of the NEAT approach could further advance research on cyclone merger. As noted in Section 1, merger typically occurs when northward and southward tracking cyclones move together. A three-dimensional extension could show whether the northward (southward) passage shown in Figure 5 is related to upper (lower) tropospheric disturbances. Because the NEAT approach can identify cyclone pathways, it may be used to calculate the momentum and heat transport of each individual cyclone system. In addition, the NEAT approach produces image shape indices allowing for comparison of eddy flux and eddy morphology, common features of dynamic meteorology.

Acknowledgements

The author would like to thank Prof. K. I. Hodges, Prof. S. Minobe, and two anonymous reviewers who provided insightful comments on improving the manuscript. Mr. K. Takatama and Mr. S. Amada helped me download the JRA25/JCDAS dataset from http://jra.kishou.go.jp/JRA-25/. The author was supported by Grants-in-Aid for Young Scientists (B) 18740293 and 21740335 of the Ministry of Education, Culture, Sports, Science, and Technology, and by the Global Environment Research Fund S-5-3 of the Ministry of the Environment, Japan. Figures were drawn using GFD-Dennou Library or Grid Application Development Software (GrADS).

References

Adachi S, Kimura F. 2007. A 36-year climatology of surface cyclogenesis in East Asia under high-resolution reanalysis data. *SOLA* **3**: 113–116.

Bengtsson L, Hodges KI, Keelyside N. 2009. Will extra-tropical storm intensity in a warmer climate?. *Journal of Climate* **22**: 2276–2301.
Blackmon ML. 1976. A climatological spectral study of the 500 mb geopotential height of the Northern Hemisphere. *Journal of Atmospheric Science* **33**: 1607–1623.
Blender R, Schubert M. 2000. Cyclone tracking in different spatial and temporal resolutions. *Monthly Weather Review* **128**: 377–384.
Dean DB, Bosart LF. 1996. Northern Hemisphere 500-hPa trough merger and fracture: a climatology and case study. *Monthly Weather Review* **124**: 2644–2671.
Hodges KI. 1994. A general method for tracking analysis and its application to meteorological data. *Monthly Weather Review* **122**: 2573–2586.
Hodges KI, Hoskins BJ, Boyle J, Thorncroft C. 2003. A general method for tracking analysis and its application to meteorological data. *Monthly Weather Review* **131**: 2012–2037.
Hoskins BJ, Hodges KI. 2002. New perspectives on the Northern Hemisphere winter storm tracks. *Journal of Atmospheric Science* **59**: 1041–1061.
Hoskins BJ, Hodges KI. 2005. New perspectives on the Southern Hemisphere winter storm tracks. *Journal of Climate* **18**: 4108–4129.
Inatsu M, Kimoto M. 2005. Two types of the interannual variability of the mid-winter storm-track and their relationship to the global warming. *SOLA* **1**: 61–64.
Lambert S. 1988. A cyclone climatology of the Canadian Climate Centre general circulation model. *Journal of Climate* **1**: 109–115.
Le Treut H, Kalnay E. 1990. Comparison of observed and simulated cyclone frequency distribution as determined by an objective method. *Atmosfera* **3**: 57–71.
Morel C, Senesi S. 2002. A climatology of mesoscale convective system over Europe using satellite infrared imagery. I: methodology. *Quarterly Journal of the Royal Meteorological Society* **128**: 1953–1971.
Murray RJ, Simmonds I. 1991. A numerical scheme for tracking cyclone centers from digital data. Part I: development and operation of the scheme. *Australian Meteorological Magazine* **39**: 155–166.
Nakamura H. 1992. Midwinter suppression of baroclinic wave activity in the Pacific. *Journal of Atmospheric Science* **49**: 1629–1642.
Ogura Y, Nishimura S, Kumabe Y. 2006. Otenki no mikata tanoshimikata (7) Part I (Written in Japanese). *Tenki* **53**: 49–54.
Onogi K, Tsutsui J, Koide H, Sakamoto M, Kobayashi S, Hatsushika H, Matsumoto T, Yamazaki N, Kamahori H, Takahashi K, Kadokura S, Wada K, Kato K, Oyama R, Ose T, Mannoji N, Taira R. 2007. The JRA-25 reanalysis. *Journal of the Meteorological Society of Japan* **85**: 369–432.
Pinto JG, Spangehl T, Ulbrich U, Speth P. 2005. Sensitivities of a cyclone detection and tracking algorithm: individual tracks and climatology. *Meteorologische Zeitschrift* **14**: 823–838.
Samet H. 1989. Connected component labeling using quadtree. *Journal of the Association for Computing Machinery* **28**: 487–501.
Sinclair MR. 1994. An objective cyclone climatology for the Southern Hemisphere. *Monthly Weather Review* **122**: 2239–2256.
Sinclair MR. 1997. Objective identification of cyclones and their circulation intensity, and climatology. *Weather Forecasting* **12**: 595–612.
Takayabu I. 1991. 'Coupling Development' : an efficient mechanism for the development of extratropical cyclones. *Journal of the Meteorological Society of Japan* **69**: 609–621.
Thorncroft CD, Hoskins BJ, McIntyre ME. 1993. Two paradigms of baroclinic-wave life-cycle behaviour. *Quarterly Journal of the Royal Meteorological Society* **119**: 17–55.
Ulbrich U, Leckebusch GC, Pinto JG. 2009. Extra-tropical cyclones in the present and future climate: a review. *Theoretical and Applied Climatology* **96**: 117–131.
van Bebber WJ. 1891. Die Zugstraßen der barometrischen Minima nach den Bahnenkarten der Deutsche Seewarte für den Zeitraum 1875–1890. *Meteorologische Zeitschrift* **8**: 361–366.
Vila DA, Machado LAT, Laurent H, Velasco I. 2008. Forecast and tracking the evolution of cloud clusters (ForTraCC) using satellite infrared imagery: methodology and validation. *Weather Forecasting* **23**: 233–245.
Wernli H, Schwierz C. 2006. Surface cyclones in the ERA-40 dataset, part I, novel identification method and global climatology. *Journal of Atmospheric Science* **63**: 2486–2507.
Xie S-P, Hanfer J, Tanimoto Y, Liu W, Tokinaga H, Xu H. 2002. Bathymetric effect on the winter sea surface temperature and climate of the Yellow and East China Seas. *Geophysical Research Letters* **29**(24): 2228.